

# Comparing Greenhouse Floor Heating Designs Using CFD

July 2005

E. Reiss, Program Associate

A.J. Both, Assistant Extension Specialist

D.R. Mears, Professor

*Bioresource Engineering, Department of Plant Biology and Pathology, Rutgers University*

## Abstract

Floor heating in greenhouses has become more and more popular over the past decades because of the considerable benefits warm floors can have on greenhouse crops. In addition, bottom watering is beneficial for many crops. Making use of the synergy of both bottom heat and bottom watering, many greenhouse growers are utilizing heated ebb and flood floors as their main plant production system. While typical warm floor systems work well, they may not be fully optimized. Accurate and flexible computer models can be extremely valuable design tools when applied to the study of greenhouse environmental control systems and can answer many questions without the time and expense associated with experimental research. A model was developed and validated, using computational fluid dynamics (CFD) software, of a typically designed warm floor system. The model was then modified to investigate the effect of heating pipe diameter and spacing, vertical position in the floor slab, and soil thermal conductivity on heat flux through the floor and temperature uniformity at the floor surface for typically designed commercial greenhouse floor heating systems. Thirty two simulations were completed to compare the performance of two different pipe diameter/spacings, two pipe elevations in the floor slab, and two soil conductivity values, each with four pipe water and greenhouse air temperature combinations. The results showed that soil thermal conductivity had little effect on temperature, heat flux, or temperature uniformity on the surface of the floor. Raising the pipe position increased both the floor surface temperature and surface heat flux, but reduced the surface temperature uniformity and had little impact on reducing soil heat flux. Using a smaller diameter pipe with a closer spacing increased the temperature, heat flux, and temperature uniformity on the surface of the floor without increasing the percentage of the total heat input to the floor that was lost to the soil below the floor.

## Introduction

According to the USDA National Agricultural Statistics Service, 36,652 ha (90,566 acres) of land were devoted to floriculture crops in 2002 (most recent data available). This included bedding/garden plants, cut flowers and cut florist greens, foliage plants, and potted flowering plants. Of that total area, nearly 25% or 9,046 ha (22,352 acres) was in greenhouses or some type of protected culture, while the balance was in outdoor production. This is a 5% increase since 1997.

For greenhouses to be economically viable they must be able to produce products with a much higher value per unit area per unit time than those grown outdoors, since much higher initial investment and operating costs are required. In order to achieve this higher value, better quality products and increased productivity is required while reducing initial and ongoing operational costs such as equipment, energy, and labor. Environmental control systems that can provide these advantages are valuable and important to the greenhouse industry. Heated ebb and flood floors are one such system that has become increasingly popular with growers because it can increase both crop production and value, while reducing initial investment and operating costs.

In addition to providing a warm root zone for the crop, the benefits of which have been well documented, bottom heat also creates a more uniform temperature environment increasing the percentage of the crop that will reach market maturity at the same time. When a greenhouse crop is grown on a warm floor, lower ambient greenhouse air temperatures can often be maintained while providing the same crop temperatures compared to a crop grown on a bench with perimeter and/or overhead heating. This reduction in bulk greenhouse air temperature results in significant reductions in energy use. The large thermal mass of the floor can also store heat and provide it to the crop in the event of a power outage or boiler failure, thereby helping to avoid costly crop losses due to these types of failures. The open space provided by these systems leads to efficient internal transport of plants throughout the greenhouse, providing increased production and labor efficiency. Space efficiency can exceed 90%, allowing the utilization of pot lifting/spacing machines that further improve labor efficiency. With bottom watering, the plant leaves never get wet, thereby reducing the potential for disease (Uva et al., 1998). Unlike other watering systems where all plants get the same amount of water regardless of their needs, this system brings all pots up to field capacity, yielding more uniformity in the crop. Finally, as there is more and more concern about contamination of our aquifers from fertilizers and pesticides, this type of floor provides almost complete containment of these compounds within the greenhouse space and continually recycles the nutrients and water used in the system conserving valuable resources. With all the advantages these floors provide, it is not surprising that their adoption by greenhouse operators is increasing.

Typically, heated ebb and flood floors consist of a concrete slab that can be flooded with up to 5.1 cm (2 in.) of water or nutrient solution. The solution is stored in holding tanks, and is pumped to the surface of the floor through a network of pipes located below the floor (Both et al 2001). Unused water is then returned to the holding tanks by gravity providing a completely closed system. The floor is flooded as needed by the particular crop or on a regular schedule. The floor heating component of the system is accomplished by embedding plastic pipe ranging from 13 mm (0.5 in) to 22 mm (0.87 in.) inside diameter in the 10.2 cm (4 in.) concrete slab. The pipe spacing is typically 22.9 cm (9 in) or 30.5 cm (12 in.) (center to center) with the smaller diameter pipe generally placed closer together. Warm water ranging from 26.7°C (80°F) to 60°C (140°F) is circulated through the pipes, while the temperature of the water delivered to the pipes is controlled by three-way or four-way mixing valves (Roberts, 1996).

While the typical design described above works well, it may not be fully optimized. For greenhouse applications, the important optimization parameters include installation cost, energy use, and, most importantly, temperature uniformity within the plant-growing environment. The design criteria that influence these parameters are pipe size, pipe spacing and depth, pipe water temperature, and the use or absence of insulation below the concrete floor. Changing design parameters in the field or in experimental set-ups in order to compare performance can be expensive and time consuming. Accurate and flexible computer models can be extremely valuable design tools when applied to the study of greenhouse environmental control systems and can answer many questions without the time and expense associated with experimental research.

The benefits of commercial and residential floor heating have also been well documented and considerable work has been performed using computer models to optimize control strategies and design parameters in non-agricultural applications (Zaheer-Uddin et al., 1997; Cho and Zaheer-Uddin, 1997 and 2002). De Mey (1980) investigated the distance between heating pipes, the vertical position of the pipes in the concrete slab, and the thickness of the slab, numerically using a boundary integral equation method.

Modeling of horticultural floor heating systems has also been performed. Kurpaska and Slipek (2000) compared various greenhouse substratum heating system designs, focusing on pipe spacing, depth, and water temperature, and their effect on temperature uniformity around the crop's roots and heat loss to the soil beneath the crop. A computer model utilizing the finite difference method was developed by Parker et al. (1981) and used to predict heat transfer in soil heated by a buried warm water pipe system.

Computational fluid dynamics (CFD) is increasingly being used as an engineering design tool to model the interaction between the internal climates of greenhouses with outside weather conditions (Reichrath and Davies, 2001). CFD was employed to study the effects of side vent opening size and location on airflow patterns and temperature distribution in naturally ventilated greenhouses (Short and Lee, 2002). Kacira et al. (2004) analyzed the effect of wind speed, side ventilators, and span numbers on ventilation rates using the CFD approach, showing that when both side and roof ventilators were used, the maximum greenhouse ventilations rate was achieved. Lee et al. (2002), used CFD models to study the effect of roof vent opening of fully open-roof style multi-span greenhouses, and validated the output with particle image velocimetry data. Montero et al. (2004) investigated nighttime heat fluxes in unheated greenhouses, using a steady state two-dimensional CFD model. The model was then used to suggest passive methods for reducing energy losses.

For the work described in this paper, CFD was used to investigate and optimize typical pipe in slab floor heating systems commonly used today. To this end, a computer model has been developed and validated that predicts the temperature distribution on the surface of a heated floor as well as the heat flux from that surface. The model was then used to evaluate the effect of pipe size, temperature, spacing, and vertical position in the concrete slab on surface temperature uniformity. How much of the heat applied to the floor reaches the greenhouse environment and how much is lost to the soil below the greenhouse was also investigated as a function of water and air temperature, pipe spacing and size, pipe elevation, and thermal conductivity of the soil.

## **Materials and Methods**

CFD software (FLUENT Inc., Lebanon, NH) was used to develop the model, and data was collected in a research greenhouse located at Rutgers University, New Brunswick, NJ to validate this model. The greenhouse was manufactured by Van Wingerden Greenhouse Company (Horse Shoe, NC) and measures 17.7m (58ft) by 18.3m (60ft). A typical ebb and flood heated floor was installed in the greenhouse using polypropylene pipe having an inside diameter of 22 mm (0.87 in.) installed on 30.5 cm (12 in.) centers in the lower third of a 10.2 cm (4 in.) concrete slab. A three way mixing valve was used to control the temperature of the water, that was heated with a gas fired boiler, and pumped through the ten pipe loops in the slab, each loop measuring approximately 110 m (360 ft) long. Any supplemental heating required to maintain the set point air temperature was provided by overhead and perimeter hot water heating pipes. A greenhouse environment controller (Argus Controls, White Rock, British Columbia) controlled all equipment required to maintain the air and water temperatures.

The model represents a 1.55 m (61 in.) wide cross section of the concrete floor, and within this section five heat pipes are incorporated (Figure 1). Within this domain, conduction, convection, and radiation heat transfer was modeled. Heat is transferred by conduction from the warm water in the pipes through the pipe walls, then through the concrete to the surface of the floor where it leaves by convection and radiation. The top surface of the model therefore was assigned a mixed boundary condition of both convection and radiation. A fixed temperature boundary condition was assigned to the water in the pipes and an adiabatic boundary condition

was assigned to the sides and bottom of the model domain. With the model's boundaries defined in this way, the temperature distribution in the concrete and heat flux from the surface could be predicted.

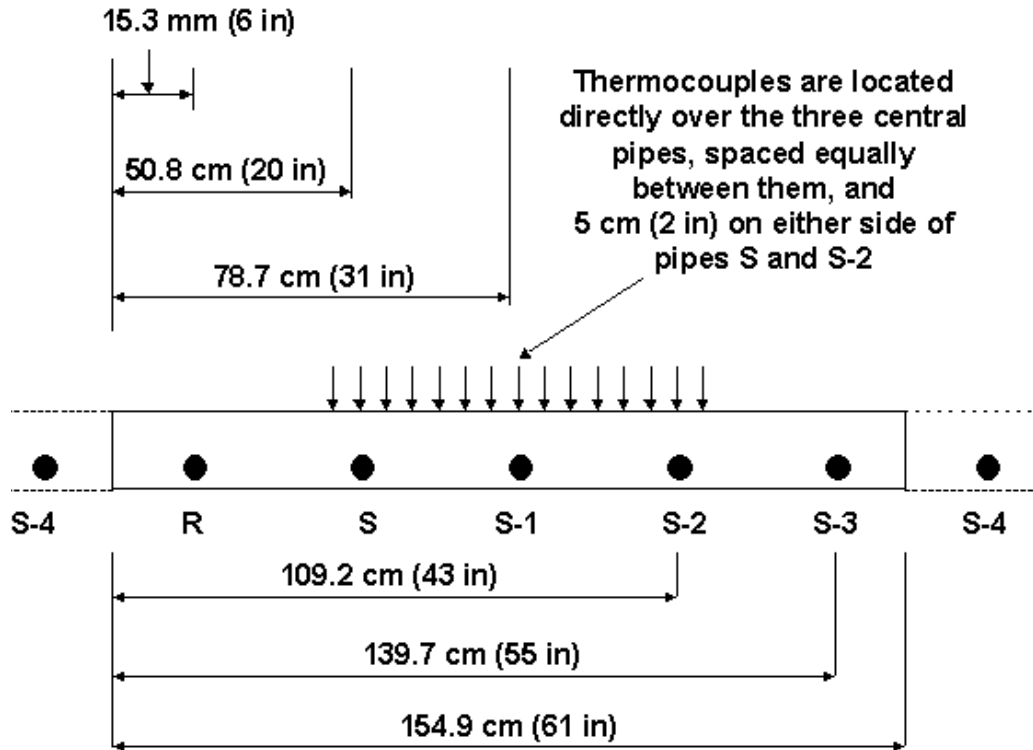


Figure 1. Cross section of the floor section used for the model (including heating pipes R through S-3), and the location of the 15 thermocouples over the three center heating pipes (R = Return, S = Supply).

Table 1 shows the materials that were defined in the model and their respective assigned properties. All properties are at standard temperature and pressure and, except for concrete, taken from the literature. Concrete has significant variation in its material properties. The thermal conductivity of concrete can vary depending on the particular concrete's density, moisture content, and material make-up. The concrete used in the research greenhouse was made with half of its cement replaced with slag (a cementitious by-product of the steel industry) in order to make it more resistant to the salts in the nutrient solution used to fertigate the crop which could potentially affect its thermal conductivity. The density of the research greenhouse concrete was measured to be  $2465 \text{ kg/m}^3$  ( $154 \text{ lb}_m/\text{ft}^3$ ), just over seven percent higher than typical values published for construction concrete (Incropera and DeWitt 1996). This is most likely a result of the concrete being vibrated during the installation process and this will increase the thermal conductivity. With the floor being flooded regularly to irrigate the crop being grown during the experimental period, the moisture content of the concrete floor could be somewhat higher than it would be otherwise. With all these variables, and without direct measurement, it is hard to know what the actual thermal conductivity was for this concrete. With the variability in the other material properties listed in Table 1 very small, and the correct thermal conductivity value for the concrete uncertain, the model was calibrated by adjusting the concrete's thermal

conductivity value until good comparison between measured and predicted temperatures was found.

Table 1. Material properties used in the simulation model.

Material	Density kg/m <sup>3</sup> (lb <sub>m</sub> /ft <sup>3</sup> )	Specific heat J/kg-K (BTU/lb <sub>m</sub> -°F)	Thermal conductivity W/m-K (BTU/hr-ft-°F)
Air	1.1614 (0.0725)	1007 (0.214)	0.0263 (0.0152)
Concrete	2465 (153.89)	880 (0.210)	2.4 (1.4)
Polypropylene	901(56.26)	1800 (0.430)	0.13 (0.0751)
Water	992 (61.93)	4178 (0.998)	0.631 (0.3646)

An area in the greenhouse was selected where the data could be collected to provide inputs to the model as well as to provide model validation data. The inputs required for the model are shown in the first four columns of Table 2. The free stream (bulk mean) air temperature was measured using a thermocouple in an aspirated chamber positioned 61 cm (24 in.) above the experimental area. Considering the concrete floor as a flat plate heated up, the convection heat transfer coefficient was calculated using empirical formulas (ASHRAE Handbook, 1985) for such cases (Equation 1).

$$h = 1.31 * (T_s - T_A)^{0.33} \quad \text{Eqn. 1}$$

Where:

- $h$  = Convection coefficient
- $T_s$  = Temperature of the floor surface (°C)
- $T_A$  = Temperature of the air (°C)

With the convection heat transfer coefficient and the free stream air temperature defined at the top boundary, the model can calculate the heat flux leaving the floor surface by convection. In order to model the radiation heat transfer from the floor, the mean radiant temperature of the environment above the floor is required. A mean radiant temperature is simply the area weighted average temperature of a group of objects. In this case, the objects are the greenhouse structure, glazing, and a portion of the sky that is “seen” through the glazing. This mean radiant temperature can also be thought of as an external radiation temperature, that is, the temperature external to the floor that the floor receives/emits radiation from/to. To measure this external radiation temperature, an infrared temperature sensor was positioned in the experimental area pointing up to the greenhouse structure, glazing, and sky. This external radiation temperature along with the emissivity of the concrete floor provides the radiative conditions required at the model’s top boundary.

### Intermediate Results

To validate the model, four water temperatures were used: 48.9°C (120°F), 43.3°C (110°F), 37.8°C (100°F), and 32.2°C (90°F). Three fixed air temperatures of 21.1°C (70°F), 18.3°C (65°F), and 15.6°C (60°F), were used yielding 12 fixed air/water combinations in the greenhouse. Table 2 shows the actual air and water temperature values measured and used as inputs for each of the twelve cases. These twelve water/air temperatures were maintained for at least two days to assure steady state conditions in the floor. Data used as inputs for, and to validate the model were taken from the early morning time period of midnight to 05:00 hr. Only days where the outside conditions during this time period were constant were used, and the

data collected and calculated during this five-hour period was averaged to one data point for each parameter.

Table 2. Input and output data (measured and predicted) for the twelve model simulations used to validate the model.

Greenhouse Air Temperature	Convection Heat Transfer Coefficient	External Radiation Temperature	Supply Water Temperature	Measured Floor Surface Temperature	Predicted Floor Surface Temperature	Error in Floor Temp Prediction	Measured Floor Surface Heat Flux	Predicted Floor Surface Heat Flux	% Error in Predicted Heat Flux
(°C)	(W/m-K)	(°C)	(°C)	(°C)	(°C)	(°C)	W/m <sup>2</sup>	W/m <sup>2</sup>	%
21.3	2.1	17.1	32.5	25.7	25.3	0.4	55.7	48.3	13.2
18.6	2.3	11.0	32.5	23.7	22.8	0.9	78.0	65.4	16.1
15.8	2.5	9.1	32.5	22.6	21.7	0.8	85.8	72.8	15.1
21.3	2.4	15.5	38.1	27.4	27.3	0.1	78.8	71.5	9.3
18.5	2.5	13.2	38.0	26.1	26.0	0.1	89.3	79.6	10.9
15.8	2.7	10.5	38.0	24.7	24.6	0.2	99.5	89.2	10.3
21.4	2.6	15.2	43.6	29.2	29.7	-0.4	98.0	91.8	6.3
18.9	2.8	14.6	43.6	28.5	28.9	-0.4	104.8	96.8	7.6
16.4	2.9	11.1	43.7	27.2	27.4	-0.2	118.3	107.9	8.8
21.2	2.8	13.4	49.3	31.1	31.2	-0.1	129.0	115.0	10.8
18.6	2.9	11.3	49.2	29.9	31.2	-1.3	135.2	115.9	14.3
16.0	3.0	9.2	49.2	28.7	29.1	-0.4	141.8	131.8	7.1
<b>Average absolute error</b>						<b>0.44</b>	<b>Average % error</b>		<b>10.8</b>

The model's output included the temperature distribution throughout the concrete as well as the heat flux off the surface. Fifteen thermocouples were epoxied just below the concrete surface at 5.1 cm (2 in.) intervals centered over three adjacent heat pipes. These three heat pipes are represented as the central three pipes in the model's domain (Figure 1). The location of the thermocouples were defined in the model so that the model's output temperatures at those points could be determined and compared to floor surface temperature data collected in the greenhouse. To determine the heat flux off the greenhouse floor, the radiation heat flux was measured by a net radiometer (Radiation and Energy Balance Systems Inc., Seattle, WA) positioned in the experimental area. The convection heat flux was calculated using Equation 1, with floor and air temperatures measured in the greenhouse. Combining the radiation and convection heat flux resulted in the total heat flux off the floor and the result was compared to the predicted heat flux from the model's output. The next three columns in Table 2 show the average of the fifteen surface temperature locations predicted by the model, the average of the fifteen measured surface temperatures in the greenhouse, and the error (measured minus predicted) in the predicted values for each case. The last three columns show the measured and calculated heat flux in the greenhouse, the predicted heat flux off the model floor surface,

and the percent error in the predicted heat flux. Equation 2 shows the method for calculating the predicted heat flux error.

$$Q_{\text{error}} = (Q_{\text{measured}} - Q_{\text{predicted}})/Q_{\text{measured}} * 100 \quad \text{Eqn. 2}$$

Where:

$Q_{\text{error}}$  = Error in predicted heat flux (%)

$Q_{\text{measured}}$  = Measured and calculated heat flux ( $\text{W}/\text{m}^2$ )

$Q_{\text{predicted}}$  = Model's predicted heat flux ( $\text{W}/\text{m}^2$ )

Figure 2 shows the fifteen predicted surface temperatures plotted with the temperatures measured in the greenhouse for the air/supply water temperature combination of 21.3/38.1°C (70.3/100.6°F).

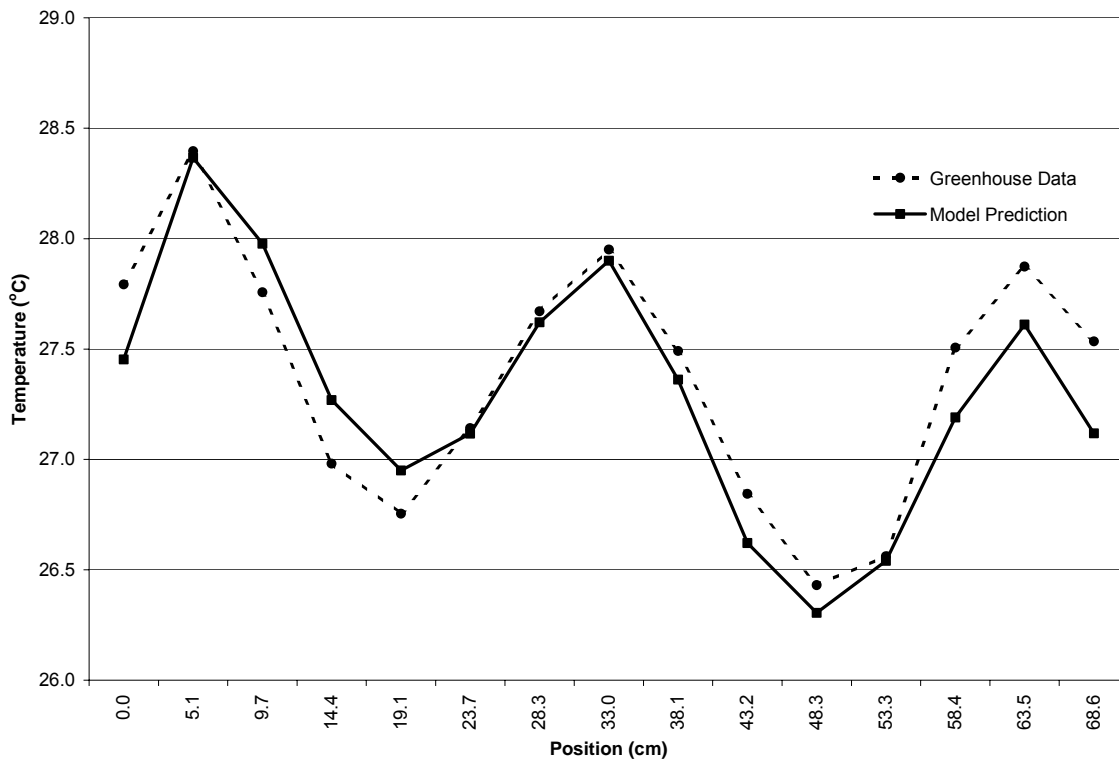


Figure 2. Fifteen surface temperatures predicted by the model along with surface temperatures measured in the greenhouse for the air/supply water temperature combination of 21.3/38.1°C (70.3/100.6 °F).

While the predicted surface temperatures did not match the measured temperatures in all cases used to validate the model as well as shown in Figure 2, the variation in temperatures across the model's top surface matched the variation in floor surface temperatures measured in the greenhouse very well. In some cases the model over or under-predicted the surface temperatures but in all but three cases the average error in predicted temperature was less than the 0.5°C error reported for the thermocouple wire used, and the overall average absolute error for all twelve cases was 0.44°C.

The heat flux predicted by the model off the slab surface was not as good as the model's temperature prediction. This could be an error in the model's heat flux calculation or an error in the way the heat flux in the greenhouse was measured or calculated, although it is believed to be most likely a model deficiency, and the cause is currently being investigated. Although the model consistently under-predicts the heat flux, the output can be used to make relative comparisons between different design parameters such as pipe size, spacing, and elevation in the slab. It can also be used to compare floor performance when different water and air temperatures are used as set points in the greenhouse.

## **Model Development**

With the model showing quite good prediction of surface temperatures, and heat flux prediction error on average less than eleven percent, investigations of pipe size, pipe spacing, and pipe elevation could be made using the model to evaluate how these design parameters impact temperature variation and heat flux. By adding a soil domain to the model, the impact of these design parameters on the amount of heat lost to the soil beneath the concrete slab could also be investigated. For these simulations, two common pipe sizes of 19 mm (0.75 in.) and 13 mm (0.5 in.) (nominal inside diameter) were used, with an industry-common spacing of 30.5 cm (12 in.) and 23 cm (9 in.), respectively. Two elevations, the bottom of the pipe 13 mm (0.5 in.) above the concrete slab bottom, and the pipe centered in the slab were compared. Two different soil thermal conductivity values were used: (0.6 W/m-K (0.35 Btu/hr-ft-°F) and 1.3 W/m-K (0.75 Btu/hr-ft-°F). Two inlet pipe water temperatures (48.9 °C, 32.2°C (120°F, 90°F)) and two air temperatures (21.1°C, 15.6°C (70°F, 60°F)) were used for each of the pipe configurations, yielding 32 simulations. Cross-linked polyethylene (PEX) pipe (a common material for heated floor systems) was modeled for all simulations, and the appropriate thermal conductivity for PEX pipe (0.38 W/m-K (0.22 Btu/hr-ft-°F)) was substituted for the polypropylene pipe used in the initial model. The appropriate thermal conductivity values listed above for soil were also incorporated for these simulations. All other material and model parameters were retained from the original model.

For the original validation simulations, the model domain represented the pipe loop configuration in the greenhouse where the data was collected. In this relatively small research greenhouse, the floor heating pipes could loop back and forth in the greenhouse three times and still be well under the 122 m (400 ft) recommended maximum loop length for that size pipe (Figure 3). In this situation, the change in temperature from one pipe to an adjacent pipe in the same loop (at the center of the house) would be only one sixth of the total change in temperature for the entire loop. Loop lengths of more than 122 m (400 ft) are not recommended so that low head losses can be maintained and less energy demanding pumps can be used. In commercial greenhouses however (typical house lengths of approximately 58 m (190 ft)), the heating pipes can only loop up and back once for 19 mm (0.75 in.) pipe while still maintaining a loop length less than 122 m (400 ft) (Figure 3). For this pipe configuration (and considering a location at the center of the house), the change in temperature from one adjacent pipe to the next is one half of the total change in water temperature for the whole loop. The simulations outlined above are intended to model typical heated floors in commercial greenhouses, and therefore the pipe configurations used in commercial greenhouses as shown in Figure 3 were modeled during simulation runs.

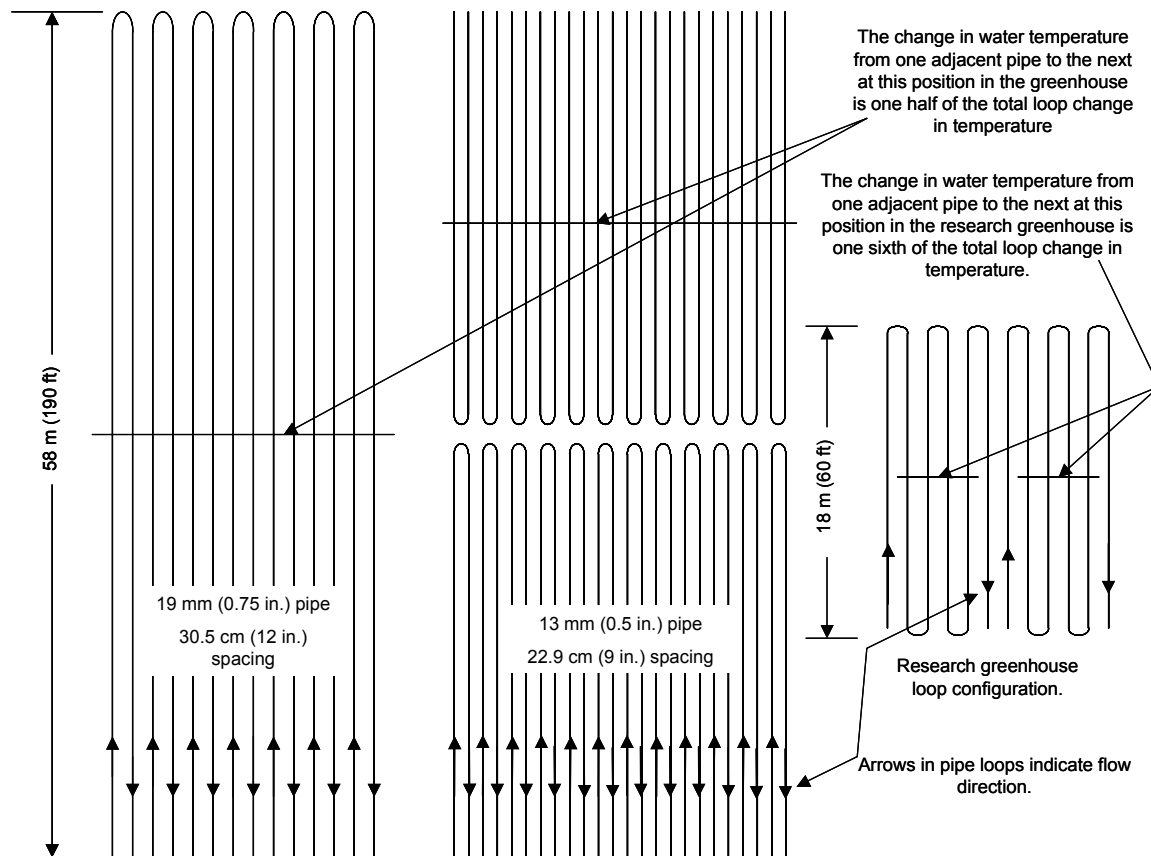


Figure 3. Common pipe configurations for 19 mm (0.75 in.) floor heating pipe on 30.5 cm (12 in.) centers (left) and 13 mm (0.5 in.) pipe on 22.9 cm (9 in.) centers (center). Also shown is the research greenhouse pipe loop configuration (right). (Drawings are not to scale)

When 13 mm (0.5 in.) pipe is used, higher head losses per unit length are incurred, so shorter loop lengths are required to maintain similar head losses compared to the 19 mm (0.75 in.) pipe. Therefore, when using 13 mm (0.5-in.) pipe in a greenhouse of this size, the heating pipes are often fed from each end of the greenhouse, thereby reducing the loop length by half. In this case as well, the delta T from one pipe to the next, is also one half the total change in water temperature for the whole loop (when considered at the locations shown in Figure 3). For all 13 mm (0.5 in) pipe simulations, the model calculations were performed at the cross sectional cut shown in Figure 3. This way, the same delta T was considered from one pipe to the next for all simulations regardless of pipe size or spacing for each of the two water temperatures considered.

For each of the two water temperatures used in the simulations, the change in temperature across the whole loop (inlet temperature to outlet temperature) was taken from data collected in the greenhouse. The same change in water temperature was used regardless of which air temperature was used during each simulation. In reality, in a greenhouse with fixed speed circulation pumps, the delta T across the loop will change as the air temperature in the greenhouse changes. Lower air temperatures increase the heat flux off the floor and increase the temperature drop across the heating loop. However, by holding the delta T constant in the simulations regardless of air temperature, the effect of water temperature, pipe spacing, pipe elevation, etc. can be evaluated without the interference of varying changes in pipe loop

temperature. An average delta T was therefore calculated and used in the simulations for each of the two water temperatures. For the 48.9°C (120°F) inlet pipe water temperature, a total loop delta T of 5.86°C (10.56°F) was used. For simulations using an inlet pipe temperature of 32.2°C (90°F), a delta T across the loop of 1.76°C (3.17°F) was used.

Five pipes were incorporated in each model's computational domain: three return pipes and two supply pipes (Figure 4). In Figure 3, the supply pipes are indicated with arrows pointing up and the return pipes with arrows pointing down. Figure 4 shows the concrete domain for the four pipe configurations used to perform the 32 simulations.

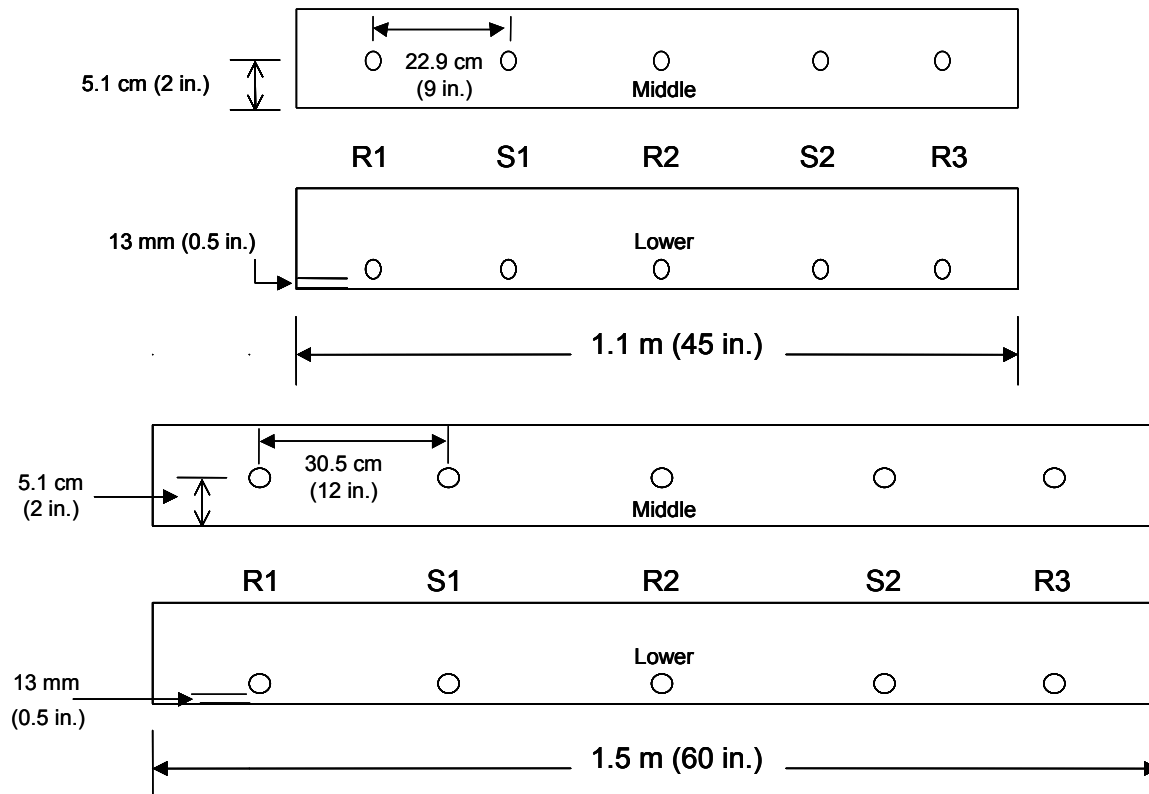


Figure 4. Concrete slab with five embedded pipes showing the four pipe configurations modeled.

Tables 3 and 4 show input and output parameters for the 32 simulations performed. Table 3 shows data for the sixteen simulations where a soil thermal conductivity of 0.6 W/m-K (0.35 Btu/hr-ft-°F) was considered, while Table 4 shows data for a soil with a thermal conductivity of 1.3 W/m-K (0.75 Btu/hr-ft-°F).

Table 3. Input and output data for simulations using soil thermal conductivity of 0.6 W/m-K (0.35 Btu/h-ft-°F).

Simulation Number	Pipe Size	Pipe Position	Supply Pipe Temperature	Return Pipe Temperature	Air Temperature	Convection Coefficient	Ext. Rad. Temperature	Avg. Surface Temperature	Surface Flux	Soil Flux	Uniformity Coefficient
	mm		°C	°C	°C	W/m <sup>2</sup> -K	°C	°C	W/m <sup>2</sup>	W/m <sup>2</sup>	
1	19	Low	32.04	31.16	21.11	1.93	13.44	24.26	61.53	5.71	0.92
2	19	Low	32.04	31.16	15.56	2.47	9.23	22.22	80.19	5.15	0.89
3	19	Low	47.75	44.82	21.11	2.87	13.44	31.56	123.73	9.33	0.88
4	19	Low	47.75	44.82	15.56	3.15	9.23	29.39	143.63	8.73	0.85
5	19	Mid	32.04	31.16	21.11	2.06	13.44	24.96	66.58	5.69	0.88
6	19	Mid	32.04	31.16	15.56	2.58	9.23	23.11	86.83	5.14	0.83
7	19	Mid	47.75	44.82	21.11	2.99	13.44	32.90	134.67	9.29	0.82
8	19	Mid	47.75	44.82	15.56	3.27	9.23	30.92	156.37	8.69	0.78
9	13	Low	32.04	31.16	21.11	2.06	13.44	24.95	66.86	6.09	0.97
10	13	Low	32.04	31.16	15.56	2.57	9.23	23.08	87.09	5.63	0.95
11	13	Low	47.75	44.82	21.11	2.98	13.44	32.85	135.06	10.06	0.95
12	13	Low	47.75	44.82	15.56	3.26	9.23	30.85	156.69	9.56	0.94
13	13	Mid	32.04	31.22	21.11	2.19	13.44	25.74	72.80	6.07	0.93
14	13	Mid	32.04	31.16	15.56	2.68	9.23	24.09	94.90	5.60	0.91
15	13	Mid	47.75	44.82	21.11	3.11	13.44	34.37	148.08	10.00	0.90
16	13	Mid	47.75	44.82	15.56	3.38	9.23	32.60	171.86	9.51	0.88

The first column in each table shows the simulation number used for easy referencing. The next two columns show the size and position of the pipe considered in each case. As mentioned earlier, the two pipe positions considered were; the bottom of the pipe positioned 13 mm (0.5 in.) above the bottom of the concrete (designated as “Low” in column three) and the pipe centered in the 10.2 cm (4 in.) high concrete slab (designated as “Mid” in column three). This is followed by the temperatures assigned to the water in the supply and return pipes. The next three columns list the parameters required to define the top boundary where convection and radiation heat transfer was modeled. The convection coefficient was determined iteratively, since the surface temperature was not known until the model’s output was completed and could be used to calculate the coefficient. First a guess was made based on experience, and then

checked using Equation #1 with the input air temperature and the output average surface temperature. Based on the error in the first guess, a new coefficient was used and checked again until the error was less than 0.1 W/m-K (0.06 Btu/hr-ft-°F). The impact of an error of 0.1 W/m-K (0.06 Btu/hr-ft-°F) was considered not significant. The two exterior radiation temperature values used were average values taken from data collected in the research greenhouse for the two corresponding air temperatures. Equation 3 was used by FLUENT to calculate the radiation heat loss of the concrete surface and an emissivity of 0.96 was used as a boundary condition parameter for the top surface of the concrete floor. (Although the model is two dimensional, the “Area” in Equation 3 was determined by the model as the simulated width with a depth of one meter.) To model the heat flux to the soil below the floor, a soil depth of 1.5 m (60 in.) was defined with a constant deep soil temperature of 12.2 °C (54 °F) assigned as a lower boundary condition to the model.

$$Q/A = \varepsilon \sigma * (T_1^4 - T_2^4) \quad \text{Eqn. 3}$$

Where:

Q = Heat transfer by radiation (W)

A = Area (m<sup>2</sup>)

σ = Stefan-Boltzman constant = 5.6697E<sup>-8</sup> W/m<sup>2</sup>K<sup>4</sup>

T<sub>1</sub> = Temperature of surface 1 (K) (i.e., the floor surface temperature)

T<sub>2</sub> = Temperature of surface 2 (K) (i.e., the external radiation temperature)

ε = Emissivity of surface 1

To determine the average surface temperature (Tables 3 and 4), locations at the top boundary (i.e., the top of the concrete floor) in each model were defined. For the 1.5 m (60 in.) wide models (Figure 4), these locations were spaced every 4.9 cm (2 in.), while for the 1.1 m (45 in.) models the interval between points was 3.7 cm (1.5 in.). With these respective spacings, some of the locations could be defined to fall directly over the center of each pipe and each model has the same number of locations defined between pipes. The average surface temperature was then calculated using the model’s output at these locations from R1 to S2 (Figure 4) for all simulations. This way, the fact that the model represents three return pipes and only two supply pipes will not impact the output since only the floor section over two return and two supply pipes was considered. Columns ten (surface flux) and eleven (soil flux) of Tables 3 and 4 show the heat flux off the top boundary of the model and the flux to the soil domain below the floor. (As a result of the unequal number of supply and return pipes in the model, there is an error of less than one percent in the model’s calculation of the surface flux.) A uniformity coefficient (UC) was calculated using Equation 4 to quantify the temperature variability across the top boundary of the model and is listed in the last column. Similarly, as for the average surface temperature calculation, only the area between pipes R1 and S2 was considered for the uniformity coefficient calculation.

$$UC = 1 - CV = 1 - \left[ \frac{\sum (Y_i - Y_{ave})^2}{(n-1) Y_{ave}} \right]^{0.5} \quad \text{Eqn. 4}$$

Where:

Y<sub>i</sub> = Temperature at location i

Y<sub>ave</sub> = Average surface temperature

n = Number of surface temperature values (n = 19)

CV = Coefficient of Variation

UC = Uniformity Coefficient (0 ≤ UC ≤ 1)

Table 4. Input and output data for simulations using a soil conductivity value of 1.3 W/m-K (0.75 Btu/h-ft-°F).

Simulation Number	Pipe Size	Pipe Position	Supply Pipe Temperature	Return Pipe Temperature	Air Temperature	Convection Coefficient	Ext. Rad. Temperature	Avg. Surface Temperature	Surface Flux	Soil Flux	Uniformity Coefficient
	mm		°C	°C	°C	W/m <sup>2</sup> -K	°C	°C	W/m <sup>2</sup>	W/m <sup>2</sup>	
17	19	Low	32.04	31.16	21.11	1.87	13.44	24.00	59.53	12.03	0.91
18	19	Low	32.04	31.16	15.56	2.44	9.23	21.99	78.38	10.85	0.88
19	19	Low	47.75	44.82	21.11	2.84	13.44	31.16	120.26	19.69	0.87
20	19	Low	47.75	44.82	15.56	3.12	9.23	29.01	140.38	18.43	0.84
21	19	Mid	32.04	31.16	21.11	2.02	13.44	24.70	64.58	11.97	0.87
22	19	Mid	32.04	31.16	15.56	2.55	9.23	22.88	85.00	10.80	0.82
23	19	Mid	47.75	44.82	21.11	2.96	13.44	32.50	131.16	19.54	0.81
24	19	Mid	47.75	44.82	15.56	3.24	9.23	30.55	153.06	18.30	0.77
25	13	Low	32.04	31.16	21.11	2.01	13.44	24.72	65.09	12.89	0.96
26	13	Low	32.04	31.16	15.56	2.55	9.23	22.87	85.40	11.91	0.95
27	13	Low	47.75	44.82	21.11	2.95	13.44	32.48	131.92	21.31	0.94
28	13	Low	47.75	44.82	15.56	3.23	9.23	30.50	153.69	20.27	0.93
29	13	Mid	32.04	31.22	21.11	2.15	13.44	25.51	71.03	12.79	0.93
30	13	Mid	32.04	31.16	15.56	2.66	9.23	23.88	93.23	11.81	0.90
31	13	Mid	47.75	44.82	21.11	3.08	13.44	34.03	144.89	21.12	0.89
32	13	Mid	47.75	44.82	15.56	3.36	9.23	32.27	168.81	20.07	0.87

## Summary of Modeling Results

### ***Soil thermal conductivity***

When comparing the columns showing average surface temperature and surface flux in Table 3 to the same columns in Table 4, we see that the two very different soil conductivities result in very similar average surface temperature and surface heat flux values. When comparing simulations 1 and 17, 2 and 18, 3 and 19, etc., there is no more than 0.4°C (0.72°F) difference in average surface temperature between any of the sixteen comparisons. The average difference for all sixteen comparisons is 0.3°C (0.54°F), with a standard deviation of 0.07°C (0.13°F).

When making a similar comparison of surface flux, there is at most a 3.2 percent decrease in the surface flux when considering a soil conductivity of 1.3 W/m-K (0.75 Btu/h-ft-°F) over a value of 0.6 W/m-K (0.35 Btu/h-ft-°F). For all sixteen comparisons, the average decrease is 2.3 percent, with a standard deviation of 0.4 percent.

When comparing the uniformity coefficient, there is again very little difference when considering a soil conductivity of 0.6 W/m-K (0.35 Btu/h-ft-°F) or 1.3 W/m-K (0.75 Btu/h-ft-°F) for comparable simulations (simulations 1 and 17, 2 and 18, 3 and 19, etc.). The largest difference in the UC is 0.01, with an average difference of 0.006. As expected however, the flux to the soil below the floor with a soil conductivity of 1.3 W/m-K (0.75 Btu/h-ft-°F) is much greater (2.1 times greater) than comparable simulations with a soil conductivity of 0.6 W/m-K (0.35 Btu/h-ft-°F).

### ***Pipe position***

When considering the effect that pipe position in the slab has on average surface temperature, we see that for all comparable simulations (1 and 5, 2 and 6, 3 and 7, etc.), the average surface temperature is higher for the middle position compared with the lower position in the slab. This difference increases as the supply water temperature increases or the delta T between the supply water and air temperature increases. Comparing simulations 1 and 5, 2 and 6, 3 and 7, and 4 and 8, (19 mm (0.75 in.) pipe) shows an increase of 0.7, 0.9, 1.3, and 1.5 °C respectively, with an overall average increase of 1.1 °C. Considering the 13 mm (0.5 in.) pipe, the same trend is found with only slightly greater differences and an overall average increase of 1.3 °C.

When evaluating the surface flux for comparable simulations, we find a fairly consistent percentage increase in surface flux from the lower position to the middle position, ranging from 8.2 percent (comparing simulations 1 and 5) to 9.49 percent (comparing simulations 28 and 32), with an overall average increase for all sixteen comparisons of 9.0 percent. Increasing the water temperature, increasing the water/air temperature delta T, decreasing the pipe size/spacing, and/or increasing the soil thermal conductivity all resulted in a larger increase in heat flux when changing the pipe location from a lower to a middle position.

There is very little effect (less than one percent decrease, with an average decrease of 0.58 percent) on the heat flux to the soil when changing the pipe position from the lower to the middle position.

When looking at the effect of pipe position on the surface temperature uniformity of the slab, it is clear that raising the pipe from the lower position to the middle position has a negative result. The percent decrease in the uniformity coefficient varies from 3.1 percent to 8.3 percent. Once again, as the water temperature increases or the water/air delta T increases, the percent decrease in the uniformity coefficient increases. Overall, the average decrease for the four

water/air temperature combinations (soil conductivity = 0.6 W/m-K (0.35 Btu/h-ft-°F)) for the 13 mm (0.5 in.) pipe is less (5.0 percent) than the 19 mm (0.75 in.) pipe (6.5 percent). The results for the simulations using a soil conductivity of 1.3 W/m-K are virtually the same.

### ***Pipe diameter/spacing***

If we compare the output of the model for 13 mm (0.5 in.) pipe on 22.9 cm (9 in.) centers vs. 19 mm (0.75 in.) pipe on 30.5 cm (12 in.) centers with a lower pipe position (simulations 1 and 9, 2 and 10, 3 and 11, and 4 and 12.), and evaluate the average surface temperature, we see that the smaller pipe on closer spacing results in a higher average surface temperature value for all comparisons. The result is almost exactly the same irrespective of soil conductivity values. The smallest difference of 0.69 °C is found when comparing simulations 1 and 9, while the largest difference of 1.46 °C is found when comparing simulations 4 and 12, with an average difference of 1.08 °C for all four water/air temperature combinations. In general, as the difference in water to air temperature increases for the four water/air temperature combinations, the difference in average surface temperature between the two pipe size/spacing increases. When making the same comparisons with the pipes in the middle position, the same trend is found but with slightly greater differences between the two pipe diameter/spacings.

When comparing the surface flux, all simulations with the smaller pipe size/spacing had greater heat flux off the surface when all other variables were the same (simulations 1 and 9, 2 and 10, 3 and 11, etc.). For the low pipe position and soil thermal conductivity of 0.6 W/m-K (0.35 Btu/h-ft-°F), the average increase in surface flux was 8.9 percent. For the middle pipe position and the same soil conductivity, the average increase was 9.6 percent. For the low and middle pipe positions, and soil conductivity equal to 1.3 W/m-K (0.75 Btu/h-ft-°F), the increases in surface heat flux was 9.4 percent and 10.1 percent respectively, with an overall average increase for all sixteen comparisons of pipe size/spacing of 9.5 percent.

The heat flux to the soil increased as well when the smaller pipe diameter/spacing was simulated, but slightly less, on a percentage basis, than the surface flux with an overall average of 8.2 percent. It is important to note that although the heat flux to the soil increased with the smaller pipe size/spacing, the percentage of total heat input to the floor that was lost to the soil below did not increase, and in fact decreased slightly.

In general, the uniformity coefficient gets lower (less uniform) as the water temperature increases or when the difference between pipe water temperature and air temperature increases. When comparing the effect that pipe size/spacing has on uniformity, the smaller pipe diameter/spacing in all comparisons has a higher uniformity coefficient. As the pipe water temperature increases or the difference in pipe water to air temperature increases, the difference in the uniformity coefficient for the two pipe diameter/spacing increases. For example, comparing simulations 1 and 9, 2 and 10, 3 and 11, and 4 to 12, with each comparison being the same except for the simulation's pipe diameter/spacing, the percent increase in uniformity from the 19 mm (0.75 in.) pipe to the 13 mm (0.5 in.) pipe is 5.4, 6.7, 8.0, and 10.6 percent respectively for these four comparisons, with an overall average increase of 7.7 percent. The same trend is found when making similar comparisons for the middle position with a slightly higher overall average increase of 9.5 percent. When considering the simulations with the higher soil conductivity, again the same trend is found, with an overall average increase of 8.1 and 9.9 for the lower and middle positions respectively for each of the four water/air temperature combinations.

## **Conclusions**

The thermal conductivity of the soil has little effect on the surface temperature, heat flux off the surface, or the variability in surface temperature. It does however have a direct impact on the heat flux to the soil below, exemplifying the importance of quantifying the soil conductivity under a particular floor heat installation so that the economic benefits of installing insulation under the floor can be fully understood.

Raising the pipe position in the simulations resulted in higher surface temperatures and surface heat fluxes, while the flux to the soil below decreased only slightly. In addition the uniformity coefficient was lower in all cases showing poorer temperature uniformity on the surface. Given these results, when temperature uniformity is important, the increase in surface heat flux will not compensate for the reduction in temperature uniformity and a lower pipe position should be used.

The simulations show that with the 13 mm (0.5 in.) pipe placed on 22.9 cm (9 in.) centers, there is an increase in both surface temperature and surface heat flux for all cases, compared to the 19 mm (0.75 in.) pipe on 30.5 cm (12 in.) centers, regardless of pipe position or soil thermal conductivity. In addition, although there is also greater heat flux to the soil below, the percentage of the total heat input to the floor that is transferred to the soil does not increase. A better uniformity coefficient was found for all comparable (same conditions except pipe size/spacing) simulations when the smaller pipe size/spacing was simulated. This difference increases as the heat flux off the surface increases (as the water/air delta T increases). A major greenhouse heating design company reports only a slight increase in cost to install 13 mm (0.5 in.) pipe placed on 22.9 cm (9 in.) centers compared to 19 mm (0.75 in.) pipe on 30.5 cm (12 in.) centers. This, along with the results of the simulations, strongly suggests that using 13 mm (0.5 in.) pipe placed on 22.9 cm (9 in.) centers will provide a more uniform temperature environment compared with using 19 mm (0.75 in.) pipe on 30.5 cm (12 in.) centers with very little increase in cost. There may be situations however, where the constraint of reduced loop lengths associated with the smaller pipe would require or justify the use of the larger pipe, particularly when uniformity is not important.

## **Future work**

The model development is continuing and improvements are being made so that the predicted heat flux compares more favorably to data collected in the greenhouse. A new model is also being developed so that the convective flow and temperature gradients in the air above the floor can be accurately modeled. With this accomplished, a crop can then be added to the model and different control strategies can be simulated for optimization.

## **Acknowledgements**

The authors would like to acknowledge the significant contribution Emily Reiss made to this work, by running simulations, extracting and organizing data, and performing literature searches.

## References

- ASHRAE. 1985. Handbook of fundamentals. American Society of Heating, Refrigerating, and Air-Conditioning Engineers. Atlanta, GA.
- Both, A.J., E. Reiss, D.R. Mears, and W.J. Roberts. 2001. Open-roof greenhouse design with heated ebb and flood floor. ASAE paper No. 01-4058. St. Joseph, Mich.: ASAE.
- Cho, S.H. and M. Zaheer-Uddin. 1997. A experimental study of multiple parameter switching control for radiant floor heating systems. *Energy, the International Journal* 24:433-444.
- Cho, S.H. and M. Zaheer-Uddin. 2002. Predictive control of intermittently operated radiant floor heating systems. *Energy Conversion and Management* 44:1333-1342.
- De Mey, G. 1980. Temperature distribution in floor heating systems. *Int. Journal Heat Mass Transfer* 23: 1289-1291
- Incropera, F.P., and D.P. DeWitt. 1996. *Introduction to Heat Transfer*. New York, N.Y.: John Wiley and Sons.
- Kacira, M., S. Sase, and L. Okushima. 2004. Effects of side vents and span numbers on wind-induced natural ventilation of a gothic multi-span greenhouse. *JARQ* 38(4): 227-233.
- Kurpaska, S., and Z. Slipek. 2000. Optimization of greenhouse substrate heating. *Journal of Agricultural Engineering Research* 76:129-139.
- Lee, I., S. Sase, L. Okushima, A. Ikeguchi, and W. Park. 2002. The accuracy of computational simulation for naturally ventilated multi-span greenhouse. ASAE paper No. 02-4012. St. Joseph, Mich.: ASAE.
- Montero, J.I., P. Monoz, A. Anton, and N Iglesias. 2004. Computational fluid dynamic modeling of nighttime energy fluxes in unheated greenhouses. Submitted to *Acta Hort*.
- Parker, J.J., M.Y. Hamdy, R.B. Curry, and W.L. Roller. 1981. Simulation of buried warm water pipes beneath a greenhouse. *Transactions of the ASAE* 24:1022-1029.
- Reichrath, S., and T.W. Davies. 2001. Using CFD to model the internal climate of greenhouses: past, present, and future. *Agronomie* 22(2002): 3-19.
- Roberts, W.J. 1996. Soil heating systems for greenhouse production. Rutgers Cooperative Extension Fact Sheet E208. 16 pp.
- Short, T.H., and I. Lee, 2002. Temperature and airflow predictions for multi-span naturally ventilated greenhouse. *Acta Hort*. 578: 141-152.
- USDA. 2002. Floriculture crops in the United States: 2002. National Agricultural Statistics Database. Washington, D.C.: USDA National Agricultural Statistics Service. Available at: [www.nass.usda.gov](http://www.nass.usda.gov). Accessed 23 April 2005.
- Uva, Wen-fei L., T.C. Weiler, and R.A. Milligan. 1998. A survey on the planning and adoption of zero runoff subirrigation systems in greenhouses. *HortScience*. 33(2): 193-196.
- Zaheer-Uddin, M., G.R. Zheng, and S.H. Cho. 1997. Optimal operation of an embedded-piped floor heating system with control input constraints. *Energy Conversion and Management* 38(7):713-725.